ORIGINAL ARTICLE

Journal of Cachexia, Sarcopenia and Muscle 2021; **12**: 1879–1896
Published online 26 October 2021 in Wiley Online Library (wileyonlinelibrary.com) **DOI:** 10.1002/jcsm.12792

Glucose 6-P dehydrogenase delays the onset of frailty by protecting against muscle damage

Coralie Arc-Chagnaud[1†], Andrea Salvador-Pascual[1,2†], Esther Garcia-Dominguez[1], Gloria Olaso-Gonzalez[1*], Angela G. Correas[1], Eva Serna[1], Thomas Brioche[3], Angele Chopard[3], Pablo J. Fernandez-Marcos[4], Manuel Serrano[5,6], Antonio L. Serrano[7], Pura Muñoz-Cánoves[5,7,8], Vicente Sebastiá[9], Jose Viña[1‡] & Mari Carmen Gomez-Cabrera[1‡]

[1]*Freshage Research Group, Department of Physiology, School of Medicine, University of Valencia, CIBERFES, Fundación Investigación Hospital Clínico Universitario/INCLIVA, Valencia, Spain;* [2]*Department of Integrative Biology, University of California, Berkeley, CA, USA;* [3]*INRAE, UMR866 Dynamique Musculaire et Métabolisme, Université de Montpellier, Montpellier, France;* [4]*Metabolic Syndrome Group - BIOPROMET, Madrid Institute for Advanced Studies - IMDEA Food, CEI UAM+CSIC, Madrid, Spain;* [5]*Catalan Institution for Research and Advanced Studies (ICREA), Barcelona, Spain;* [6]*Institute for Research in Biomedicine (IRB Barcelona), Barcelona Institute of Science and Technology (BIST), Barcelona, Spain;* [7]*Department of Experimental and Health Sciences, University Pompeu Fabra and CIBERNED, Barcelona, Spain;* [8]*Spanish National Center on Cardiovascular Research (CNIC), Madrid, Spain;* [9]*Clinica Ypsilon de medicina física y rehabilitación, Valencia, Spain*

Abstract

Background Frailty is a major age-associated syndrome leading to disability. Oxidative damage plays a significant role in the promotion of frailty. The cellular antioxidant system relies on reduced nicotinamide adenine dinucleotide phosphate (NADPH) that is highly dependent on glucose 6-P dehydrogenase (G6PD). The G6PD-overexpressing mouse (G6PD-Tg) is protected against metabolic stresses. Our aim was to examine whether this protection delays frailty.

Methods Old wild-type (WT) and G6PD-Tg mice were evaluated longitudinally in terms of frailty. Indirect calorimetry, transcriptomic profile, and different skeletal muscle quality markers and muscle regenerative capacity were also investigated.

Results The percentage of frail mice was significantly lower in the G6PD-Tg than in the WT genotype, especially in 26-month-old mice where 50% of the WT were frail vs. only 13% of the Tg ones ($P < 0.001$). Skeletal muscle transcriptomic analysis showed an up-regulation of respiratory chain and oxidative phosphorylation ($P = 0.009$) as well as glutathione metabolism ($P = 0.035$) pathways in the G6PD-Tg mice. Accordingly, the Tg animals exhibited an increase in reduced glutathione (34.5%, $P < 0.01$) and a decrease on its oxidized form (−69%, $P < 0.05$) and in lipid peroxidation (4-HNE: −20.5%, $P < 0.05$). The G6PD-Tg mice also showed reduced apoptosis (BAX/Bcl2: −25.5%, $P < 0.05$; and Bcl-xL: −20.5%, $P < 0.05$), lower levels of the intramuscular adipocyte marker FABP4 (−54.7%, $P < 0.05$), and increased markers of mitochondrial content (COX IV: 89.7%, $P < 0.05$; Grp75: 37.8%, $P < 0.05$) and mitochondrial OXPHOS complexes (CII: 81.25%, $P < 0.01$; CIII: 52.5%, $P < 0.01$; and CV: 37.2%, $P < 0.05$). Energy expenditure (−4.29%, $P < 0.001$) and the respiratory exchange ratio were lower (−13.4%, $P < 0.0001$) while the locomotor activity was higher (43.4%, $P < 0.0001$) in the 20-month-old Tg, indicating a major energetic advantage in these mice. Short-term exercise training in young C57BL76J mice induced a robust activation of G6PD in skeletal muscle (203.4%, $P < 0.05$), similar to that achieved in the G6PD-Tg mice (142.3%, $P < 0.01$).

Conclusions Glucose 6-P dehydrogenase deficiency can be an underestimated risk factor for several human pathologies and even frailty. By overexpressing G6PD, we provide the first molecular model of robustness. Because G6PD is regulated by pharmacological and physiological interventions like exercise, our results provide molecular bases for interventions that by increasing G6PD will delay the onset of frailty.

Keywords Aging; Antioxidant; Mitochondria; Disability; Healthspan; NADPH; Reactive oxygen species

Received: 29 September 2020; Revised: 26 July 2021; Accepted: 23 August 2021
**Correspondence to: Gloria Olaso-Gonzalez, Department of Physiology, School of Medicine, University of Valencia, Av. Blasco Ibañez 15, 46010 Valencia, Spain. Phone: +34963983266, Email: gloria.olaso@uv.es*
†These two authors have contributed equally to the work.
‡These two authors have contributed equally as senior authors of this work.

Introduction

Frailty is a clinical geriatric syndrome characterized by a cumulative decline in multiple body systems that is associated with high vulnerability to stressors, which results in a dysregulation of multiple physiological systems. If left untreated, it progresses to disability, with enormous personal and social consequences for the patients, their caretakers, and society in general.[1]

Importantly, old age, although associated to frailty, does not define frailty itself. Despite advanced age, some persons remain vigorous, while others have gradual functional decline in the absence of apparent diseases.[2] A person who is not pre-frail or frail is considered robust. In this sense, robustness is opposed to frailty.

In our study, we aimed at delaying the onset of frailty in its generally accepted broader geriatric context.[3]

Age-associated damage is of low intensity, but its chronic nature eventually leads to a global decline in the biological reserve and in cellular functionality.[4] The correlation between oxidative damage and frailty, and its mitochondrial root, has been reported in both human[5,6] and animal studies.[7,8] This led us to formulate the 'free radical theory of frailty'.[2] This theory postulates that frailty is associated with oxidative stress that acts in a dual mode: firstly, it affects the redox signalling balance that occurs in normal physiology, and secondly, if oxidative stress persists, it causes a permanent damage that provokes a failure of cell functions, especially those involved in homeostasis, that finally leads to the onset of frailty.[2]

Glucose 6-P dehydrogenase (G6PD) is the rate-limiting enzyme in the pentose phosphate pathway (PPP) and is ubiquitously expressed in mammalian tissues.[9] Glucose can be catabolized via the glycolytic pathway or via the oxidative PPP to make nicotinamide adenine dinucleotide phosphate (NADPH), the ultimate donor of reductive power for the large majority of reactive oxygen species (ROS)-detoxifying enzymes. Thus, G6PD plays a central role in the antioxidant defence.[10] Importantly, overexpression of G6PD in *Drosophila melanogaster*[11] and mice[12] leads to higher levels of NADPH and lower levels of ROS-derived damage concomitant with extended lifespan. Accordingly, G6PD deficiency, the most common human enzyme defect, is effectively managed in the clinical practice by avoiding oxidative stress.[13] Because NADPH is at the core of the anti-ROS defence, we hypothesized that an increase in G6PD activity could protect against age-associated damage and delay the onset of frailty.

To the best of our knowledge, a molecular model of vigorousness has not yet been described. Although it has been shown that life-long overexpression of HSP70[14] and the growth hormone receptor knockout (GHR-KO) mice[15] facilitate recovery after damage in muscles of old mice and enhance neuromusculoskeletal healthspan, frailty was not determined in those studies.

Here, we propose a new molecular model for the promotion of robustness, that is, the G6PD-Tg. We have characterized this mouse line[9,12] and have found lower levels of ROS-derived damage and better protection against metabolic stresses.

Using our previously described test to evaluate frailty,[16,17] we now show that overexpression of G6PD in mice results in a significant delay in frailty. This opens up room for intervention because by promoting G6PD expression, one can delay the onset of frailty in animals and hopefully in human beings.

The activation of the G6PD by nutritional[18] or pharmacological interventions[19,20] could have translational potential in geriatrics and in gerontological research. In fact, we report here that a physiological intervention, exercise training in C57BL/6J mice, induces an increase in the activity of G6PD in the skeletal muscle of an order of magnitude very similar to that obtained in the G6PD-Tg animals.

Our results reinforce the importance of pursuing frailty studies in humans with G6PD deficiency, an enzymopathy affecting over 400 million people in the world.

Materials and methods

Experimental animals

The animal study was approved by the University of Valencia Ethics Committee for Research and Animal Welfare (License References A1444079171882 and A1481561216420). Animals were housed at the Animal House Core Facility of the University of Valencia.

Cohorts of old (18–26 months) C57BL6 [wild-type (WT)] and G6PD-Tg mice were used to longitudinally evaluate frailty. Each frailty criteria had a designated cut-off point to identify the percentage of mice with the lowest performance. See references[16,17] for details.

Young (7-month-old) and old (19- to 26-month-old) C57BL6 and G6PD-Tg mice were used to study the skeletal muscle regeneration capacity.

All the molecular and biochemical determinations were performed in 21- to 27-month-old WT and G6PD-Tg mice.

High-resolution respirometry was measured in fibre bundles in ~20-month-old WT and G6PD-Tg animals.

Very old (34-month-old) WT and G6PD-Tg mice were used to quantify the skeletal muscle fibre size in basal conditions. The exercise training experiments were performed in young C57BL/6J animals (5-month-old).

Frailty score

A score for frailty was determined at 18- to 20-month-old (WT n = 24, Tg n = 39–40), 21- to 22-month-old (WT n = 17, Tg n = 36), 23- to 24-month-old (WT n = 12–14, Tg n = 28–29),

and 25- to 26-month-old (WT *n* = 5–11, Tg *n* = 16–24) animals. Briefly, we evaluated five functional parameters: body weight, motor coordination, grip strength, running time, and speed during a treadmill test. This score was fully described previously by our research team[16] and others.[17]

Muscle regeneration experiments

The skeletal muscle regeneration was studied in control (WT *n* = 4; Tg *n* = 4) and at 4 days (WT *n* = 4, Tg *n* = 4 young; WT *n* = 4, Tg *n* = 6 old animals), 7 days (WT *n* = 4, Tg *n* = 4 young; WT *n* = 3, Tg *n* = 5 old animals), and 10 days (WT *n* = 4, Tg *n* = 4 young; WT *n* = 3, Tg *n* = 4 old animals) following cardiotoxin-induced injury as previously described.[21]

Histology and immunohistochemistry in muscle cryosections

Gastrocnemius and tibialis anterior muscles were used for the analyses. Muscle samples were included in optimal cutting temperature compound (OCT), frozen in isopentane cooled with liquid nitrogen, and stored at −80°C until analysis. Transverse serial cross-sections (10 μm thick) were obtained using a cryostat maintained at −25°C (HM-560, Microm H) and mounted onto glass microscope slides. Cryosections were coloured with haematoxylin–eosin (HE) solution or immunostained using anti-eMHC antibody (F1.652, Developmental Studies Hybridoma Bank) (see Supporting Information for details).

Digital image acquisition and processing

Muscle sections were photographed with Axiovison software and were digitalized with the microscopic preparation scanner Panoramic Midi 3 (3DHISTECH Ltd., Budapest, Hungary) at ×20 magnification. Digitalization was performed with a PNG lossless high-compressed format due to the vast number of pixels scanned. Panoramic viewer (3DHISTECH Ltd.) was used for exporting all images in compressed JPEG (90% quality vs. compression ratio). To quantify myofibre size, at least 300 representative fibres of each sample were outlined, and their cross-sectional area was determined using ImageJ software (see Supporting Information for details).

RNA extraction and whole transcriptomic analysis

Total RNA from the quadriceps muscle was extracted using the TRIzol reagent. RNA integrity number (RIN) was tested by the 2100 Bioanalyzer (Agilent Technologies, Santa Clara, CA, USA), and the RNA concentration was determined by measuring absorbance at 260 nm using a spectrophotometer (GeneQuant, GE Healthcare Biosciences). Ten microarrays were analysed: WT (*n* = 5) and G6PD-Tg (*n* = 5). To determine global differences in genetic profiles between groups, principal component analysis (PCA) and unsupervised hierarchical clustering using the Partek software were performed (see Supporting Information for details).

Real-time polymerase chain reaction analysis

We isolated total RNA from the quadriceps muscle of sedentary resting (*n* = 5) and trained mice for 5 days (*n* = 7), and we performed an analysis by single real-time reverse-transcription polymerase chain reaction (RT-PCR) using TaqMan® Gene Expression Assays probes (Applied Biosystems®, Foster City, CA, USA) according to the manufacturer's recommendations (see Supporting Information for details).

GSH and GSSG determination

We determined GSH and GSSG concentrations in gastrocnemius muscles by a spectrophotometric procedure that uses *N*-ethylmaleimide (NEM) to minimize thiol auto oxidation during sample preparation.[22]

Lipid peroxidation determination by high-performance liquid chromatography

Malondialdehyde (MDA) levels were determined in gastrocnemius samples as described previously[23] (see Supporting Information for details).

Carbonylated proteins

Immunoblot detection of protein carbonyl groups in gastrocnemius samples was assessed using the 'Oxyblot Protein Oxidation Detection Kit' (Millipore, USA) (see Supporting Information for details).

Western blotting

Gastrocnemius samples were homogenized in 10 volumes of lysis buffer and centrifuged at 10 000 *g* for 10 min (4°C). Sixty micrograms of protein extract were loaded into Stain-Free 4–20% precast gels (4568095; Bio-Rad) before electrophoretic migration and transfer onto nitrocellulose membranes (Bio-Rad; Trans-Blot Turbo Blotting System). Then, the membranes were blocked and incubated overnight at 4°C with primary antibodies. The membranes were then incubated

for 1 h with a peroxidase-conjugated secondary antibody (see Supporting Information for details).

High-resolution respirometry

Mitochondrial respiration was carried out with permeabilized muscle fibre bundles from the soleus muscle of ~20-month-old G6PD-Tg (n = 4) and WT mice (n = 6) using the Oxygraph-2k (see Supporting Information for details).

In vivo metabolic assessment

Respiratory metabolism and spontaneous activity and rearing were assessed by indirect calorimetry with the OxyletPro System (Panlab, Harvard Apparatus) in ~20-month-old G6PD-Tg (n = 5) and WT mice (n = 5). Mice were single housed with ad libitum access to food and water and maintained at 20–22°C under a 12:12 h light:dark cycle (light period 08.00–20.00). All mice were acclimated to monitoring cages for 16–18 h prior to recording. Oxygen consumption was determined by measuring oxygen concentration in air entering the chamber compared with air leaving the chamber. Measurement in each chamber was recorded for 1 min at 5 min intervals for a total of 48 h.

Body composition

Mice (~20-month-old) body composition (bone mineral density, lean mass, fat mass, and fat in tissue) was analysed with simple anaesthesia using the method of dual-energy X-ray absorptiometry (DXA) with Medikors' InAlyzer (WT n = 6, Tg n = 5).

Haematological measurements

We used the veterinary 'Hematology ELEMENT HT5' and the 'Skyla VB1' analyser to provide haematological and biochemical parameters in whole EDTA blood in ~20-month-old G6PD-Tg (n = 6) and WT mice (n = 8) (Supporting Information, *Table* S1).

Exercise training

Young C57Bl/6J mice (5-month-old) were allocated in two different groups: sedentary resting mice (n = 5) and trained mice for 5 days (n = 7). Mice were trained for five consecutive days with the following protocol: treadmill downhill running (−20°) at 10 m/min for 5 min, followed by 25 min at 18 m/min (PanLab Harvard Apparatus, Columbus Instruments LE8708). After 2 days of resting, quadriceps muscles were collected.

Glucose 6-P dehydrogenase activity

Glucose 6-P dehydrogenase activity was determined as described previously[24] in quadriceps muscle samples of young trained and sedentary resting mice as well as in old WT and G6PD-Tg animals (~20-month-old).

Statistical methods

Values are expressed as the mean ± standard deviation (SD). Normal distribution of the samples was assessed by the Shapiro–Wilk test. To compare two different groups, the unpaired Student's t-test was used, or the Mann–Whitney test in case of a non-normal distribution. To study two independent variables, a two-way analysis of variance (ANOVA) test was used. For the frailty score and its criteria, differences were tested using the Pearson's χ^2 test. A one-way ANOVA was used to determine differences in gene expression between groups. The effect size in the percentage of muscle weight lost with age has been determined performing an F-test. Statistical analysis was performed using Statistica, SPSS, or GraphPad Prism software, with a significance level set at $P < 0.05$, and all graphs were represented with GraphPad Prism8 Software.

Results

Old G6PD-Tg mice are less frail than their wild-type congeners

Using a cohort of female mice (WT and G6PD-Tg) aged 18 to 26 months, we established a frailty score based on the evaluation of five parameters: body weight, motor coordination, maximal grip strength, running time, and running speed achieved during a treadmill test.[16,17]

Body weight

Mice were weighted every 2 months from 18 to 26 months of age (Supporting Information, *Figure* S1). To evaluate the loss of weight with aging, we used the mean body weight of the animals at the age of 18 months as initial controls. An animal was considered as frail for this criterion when at any given age, it had lost more than 5% of its weight at the age of 18 months. Compared with the WT, G6PD-Tg mice maintained better their weight with advancing age. At 25–26 months of age, more than 72% of WT mice were considered as frail for this criterion, whereas only 17% in the Tg group was (*Figure* 1A).

Motor coordination

The tightrope test was used to evaluate motor coordination in mice. The animals that failed the test were considered as frail for this criterion (*Figure* S1). The G6PD-Tg animals clearly performed better than the WT at the different ages tested. However, the differences only reached statistical significance in the 18- to 20- and 23- to 24-month-old mice. In the WT group, 29% and 42% of the mice failed the test at these specific ages. Only the 2.5% and 6.9% of the G6PD-Tg mice failed the motor coordination test at 18–20 and 23–24 months of age (*Figure* 1B).

Grip strength

Maximal grip strength was recorded using the grip strength metre, which detects the peak force applied on the device. The values obtained were divided by animal's body weight. G6PD-Tg mice were stronger than WT mice, especially when they were 23–24 months old (mean scores of 3.9 ± 0.2 in the WT group vs. 5.0 ± 0.1 in the G6PD-Tg group) (*Figure* S1). Consequently, 50% of the WT animals fulfilled this frailty criterion compared with the 6.9% of the same age G6PD-Tg mice (*Figure* 1C).

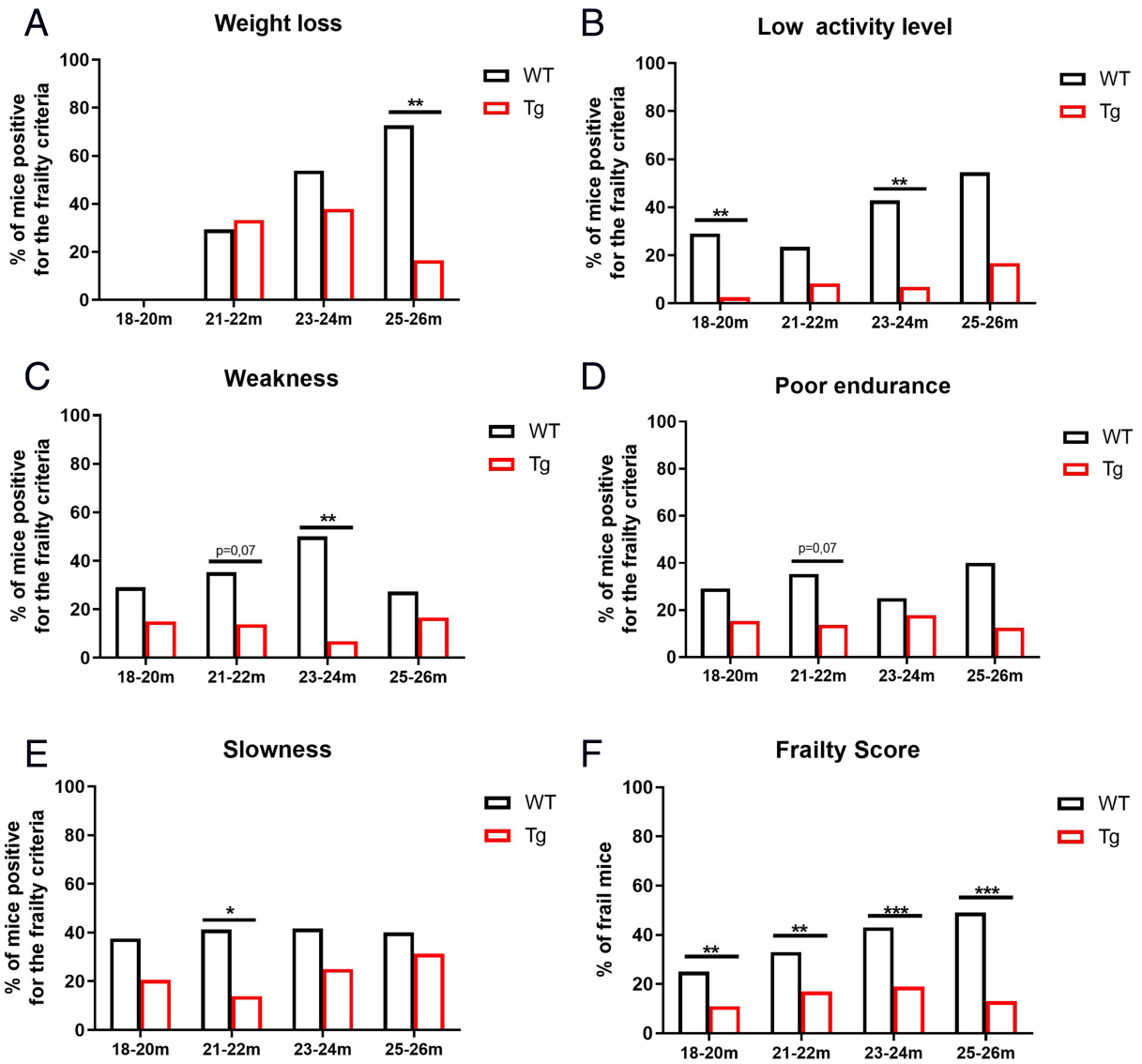

Figure 1 Valencia Score for frailty in WT and G6PD-Tg mice. (*A–E*) Percentage of mice considered as frail for each of the five parameters tested in the WT and G6PD-Tg groups (*A–E*). (*F*) The frailty score was calculated as follows: number of tests failed divided by the total number of tests performed, for each group of mice and ages. Mice were tested at different ages: 18- to 20-month-old (n = 24 WT, n = 39–40 Tg), 21- to 22-month-old (n = 17 WT, n = 36 Tg), 23- to 24-month-old (n = 12–14 WT, n = 28–29 Tg), and 25- to 26-month-old (n = 5–11 WT, n = 16–24 Tg). Statistical significance was assessed using Pearson's χ^2 test. *$P < 0.05$; **$P < 0.01$; ***$P < 0.001$.

Running time

Mice performed an incremental treadmill test until exhaustion to evaluate their endurance capacity (*Figure* S1).[3] We first determined the maximal running time achieved by the animals at the end of the test. We did not find any significant difference in this frailty parameter between the two groups of mice independently of age. Although a tendency was found in the 21- to 22-month-old animals (P = 0.07), the differences between the groups did not reach statistical significance (*Figure* 1D).

Running speed

The maximal running speed achieved at the end of the incremental test was also recorded (*Figure* S1). Slowness is an important component when evaluating frailty in the clinical practice.[3] G6PD-Tg animals were significantly faster than the WT ones when they were 21–22 months old ($P < 0.05$). At this specific age, we found that 41% of the WT mice fulfilled the frailty criterion of slowness while only 13.8% of G6PD-Tg mice did (*Figure* 1E).

Frailty score

We established a score for frailty based on the results obtained in each of the five parameters measured.[16,17] In each age group, we divided the total number of tests failed by the total number of tests performed, and we obtained the percentage of mice considered as frail. At each age range (from 18 to 26 months old), the G6PD-Tg mice were less frail than the WT. The most convincing difference was found in the older mice (25–26 months), where almost half of the WT mice were frail vs. only 13% in the G6PD-Tg group (*Figure* 1F).

Regenerative capacity of muscle stem cells in G6PD-Tg vs. wild-type animals

The activity of G6PD increases dramatically during the regeneration of skeletal muscle,[25] a process highly dependent on satellite cells.[26] Thus, we analysed the regenerative capacity of satellite cells in young WT and Tg animals in response to cardiotoxin-induced muscle injury. We found a loss of the muscle architecture in the injured tibialis anterior muscle at 4 days post-injury, due to the necrosis of myofibres and the activation of an inflammatory response (data not shown). The cross-sectional area of the newly forming myofibres at 7 and 10 days post-injury in both WT and G6PD-Tg mice was lower than in basal conditions, as expected in regenerating, not fully matured myofibres (*Figure* 2A). The frequency distribution of regenerating fibres by size was not different between G6PD-Tg and WT mice (*Figure* 2B). Signs of advanced muscle regeneration, as indicated by the appearance of large central-nucleated fibres, can be seen in *Figure* 2C. All those changes confirmed that the cardiotoxin injection was effective in the induction of muscular damage followed by regeneration.[26] The expression of embryonic myosin heavy chain (eMHC), an early marker of muscle regeneration, indicates new myofibre formation.[26] Newly regenerating myofibres were stained with an anti-eMHC antibody at 4 days post-injury (*Figure* 2F). No significant differences were found between WT and G6PD-Tg mice in the size of positive myofibres for eMHC staining ($eMHC^+$) (*Figure* 2D) or in the frequency distribution according to their size (*Figure* 2E). However, the observed trend of increased $eMHC^+$ fibre size in young Tg animals, together with the fact that frailty is a geriatric syndrome, prompted us to undertake a further study in old mice.

As in young animals, we did not find significant differences in myofibre cross-sectional area between WT and G6PD-Tg old mice at 7 or 10 days post-injury (*Figure* 3A). The frequency distribution of fibre size was not significantly different between the groups either (*Figure* 3B). Signs of advanced muscle regeneration are shown in *Figure* 3C. Newly regenerating myofibres in tibial anterior muscles were positive for eMHC expression at 4 days post-injury (*Figure* 3F). As reported in young animals, no significant differences were found between WT and G6PD-Tg old mice in $eMHC^+$ fibre size (*Figure* 3D) or in the frequency of distribution according to their size (*Figure* 3E).

Transcriptomic analysis

We performed a global gene expression analysis in skeletal muscle and found a different expression pattern between G6PD-Tg vs. WT animals. *Figure* 4A shows the PCA in G6PD-Tg and WT muscle samples according to their transcriptome. The PCA score plot showed a 47% variability between the G6PD-Tg and WT groups, and two different clustered groups could be therefore clearly appreciated.

The transcriptomic analysis showed 1653 differentially expressed genes. Of these, 779 genes were up-regulated (47%) and 874 were down-regulated (53%) in the Tg animals when compared with WT. The different pattern of gene expression observed in the PCA was confirmed by dendrogram from unsupervised hierarchical clustering analysis. *Figure* 4B shows in blue and red the statistically significant down-regulated and up-regulated genes, respectively. WT mice are clustered in the upper zone, and G6PD-Tg mice are clustered in the lower zone. Differentially expressed genes were analysed using the Pathway Studio software. The most representative metabolic pathways identified, in terms of enrichment P value, were as follows: (i) the mitochondrial respiratory chain and oxidative phosphorylation (P value 0.009, nine genes up-regulated in the G6PD-Tg vs. WT) (*Figure* 4C) and (ii) the glutathione metabolism pathway (P value 0.035, nine genes up-regulated and two genes down-regulated in the G6PD-Tg vs. WT) (*Figure* 4D). Two

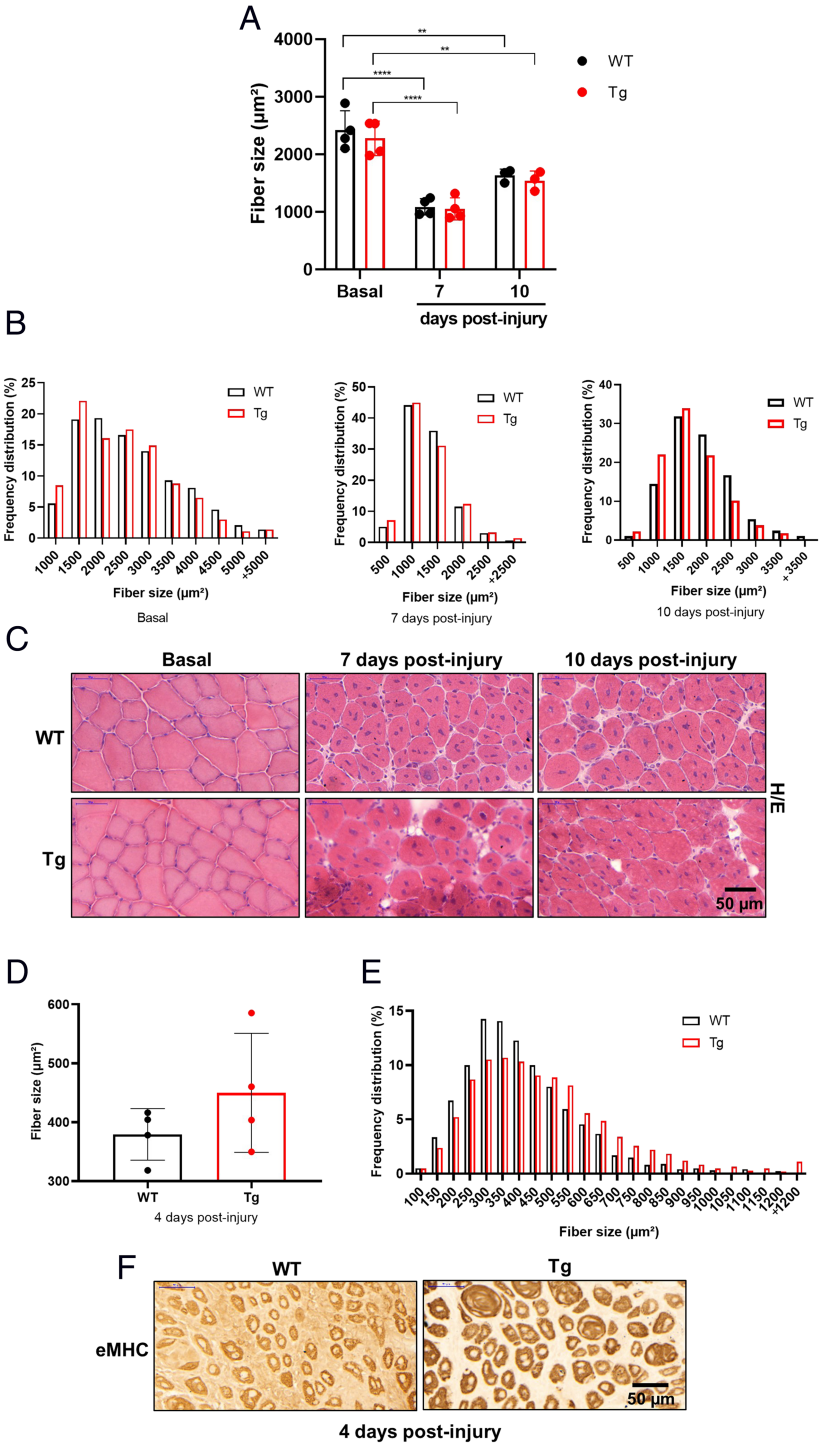

Figure 2 Tibialis anterior muscle regeneration in young WT and G6PD-Tg mice. (*A*) Quantification of the myofibre size, evaluated by the cross-sectional area, in TA muscle sections in basal conditions and regeneration at 7 and 10 days after cardiotoxin-induced injury in 7-month-old mice (n = 4 WT; n = 4 Tg, for each group). (*B*) Quantification of fibre cross-sectional area frequency of distribution in muscle sections in basal conditions and regeneration at 7 and 10 days after cardiotoxin-induced injury (n = 4 WT; n = 4 Tg, for each group). (*C*) Representative images of haematoxylin–eosin staining. (*D*) Quantification of the eMHC^{+} myofibre size, evaluated by the cross-sectional area, in tibial anterior sections in regeneration at 4 days after cardiotoxin-induced injury (n = 4 WT; n = 4 Tg, for each group). (*E*) Quantification of eMHC^{+} fibre cross-sectional area frequency of distribution (n = 4 WT; n = 4 Tg, for each group). (*F*) Representative images of eMHC immunostaining. Scale bars, 50 µm. Data bars represent mean ± SD. Dots represent individual data. Statistical significance was assessed using the two-way ANOVA test: $^{**}P < 0.01$, $^{****}P < 0.0001$.

DOI: 10.1002/jcsm.12792

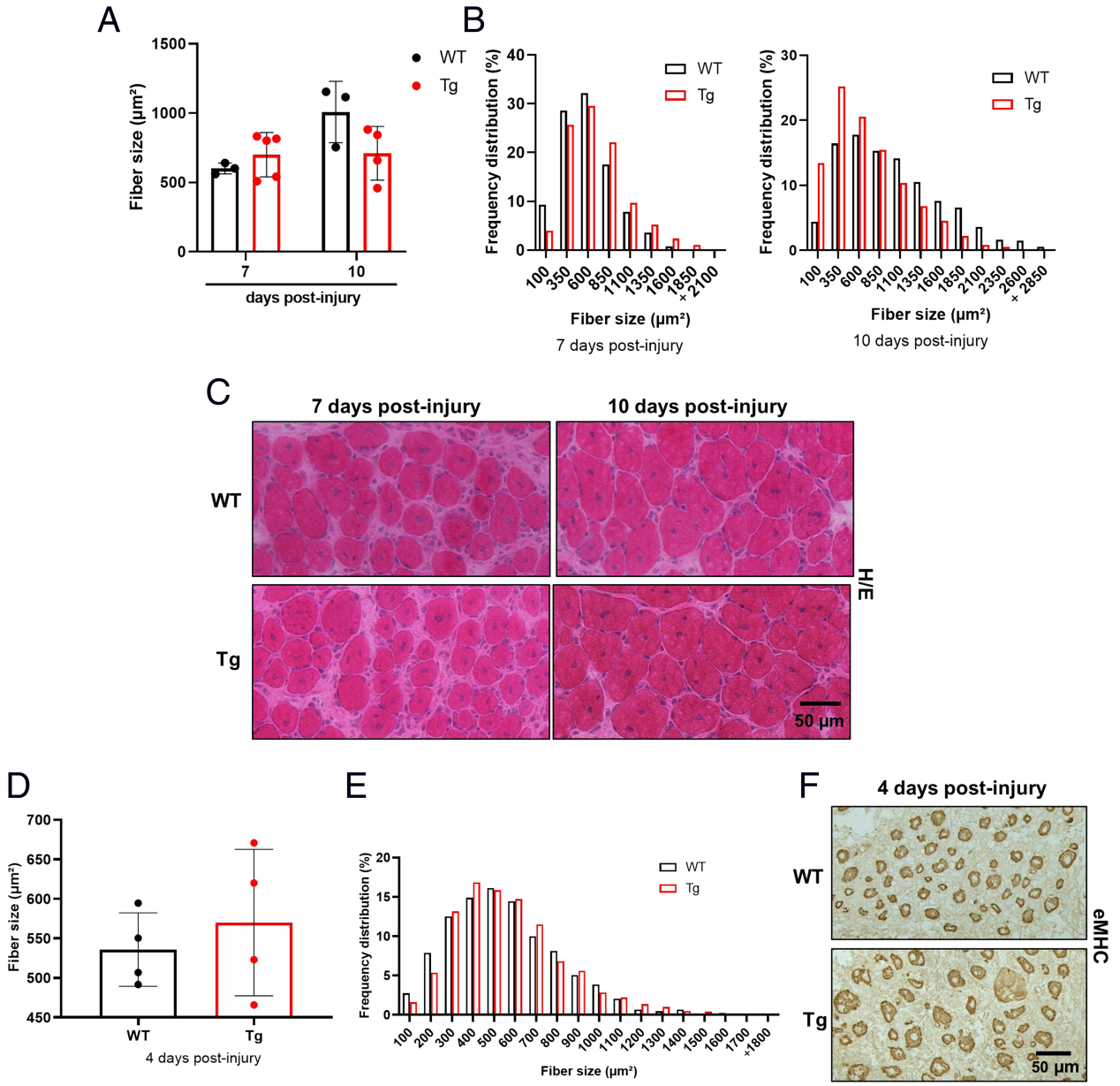

Figure 3 Tibialis anterior muscle regeneration in old WT and G6PD-Tg mice. (*A*) Quantification of the myofibre size, evaluated by the cross-sectional area, in tibial anterior muscle sections in regeneration at 7 and 10 days after cardiotoxin-induced injury (19- to 26-month-old) (n = 3 WT; n = 5 Tg and n = 3 WT; n = 4 Tg, respectively). (*B*) Quantification of fibre cross-sectional area frequency of distribution in tibial anterior sections in regeneration at 7 and 10 days after cardiotoxin-induced injury (n = 3 WT; n = 5 Tg and n = 3 WT; n = 4 Tg, respectively). (*C*) Representative images of haematoxylin–eosin staining. (*D*) Quantification of the eMHC^{+} myofibre size, evaluated by the cross-sectional area, in tibial anterior sections in regeneration at 4 days after cardiotoxin-induced injury (n = 4 WT; n = 6 Tg). (*E*) Quantification of eMHC^{+} fibre cross-sectional area frequency of distribution (n = 4 WT; n = 6 Tg). (*F*) Representative images of eMHC immunostaining. Scale bars, 50 µm. Data bars represent mean ± SD. Dots represent individual data.

relevant biological processes were also identified: (i) apoptosis (P value 3.53 × 10^{-7}, 26 genes down-regulated and 30 genes up-regulated in the G6PD-Tg vs. WT) (*Figures* 4E and S2) and (ii) the oxidative stress response (P value 5.08 × 10^{-7}, 7 genes down-regulated and 13 up-regulated in the G6PD-Tg vs. WT) (*Figure* 4F). The heatmap for the fold-change values of differently expressed genes for *Figure* 4C–4E is available in the centre of the figure.

The complete lists of the genes involved in these metabolic pathways and biological processes are shown in *Table* S2.

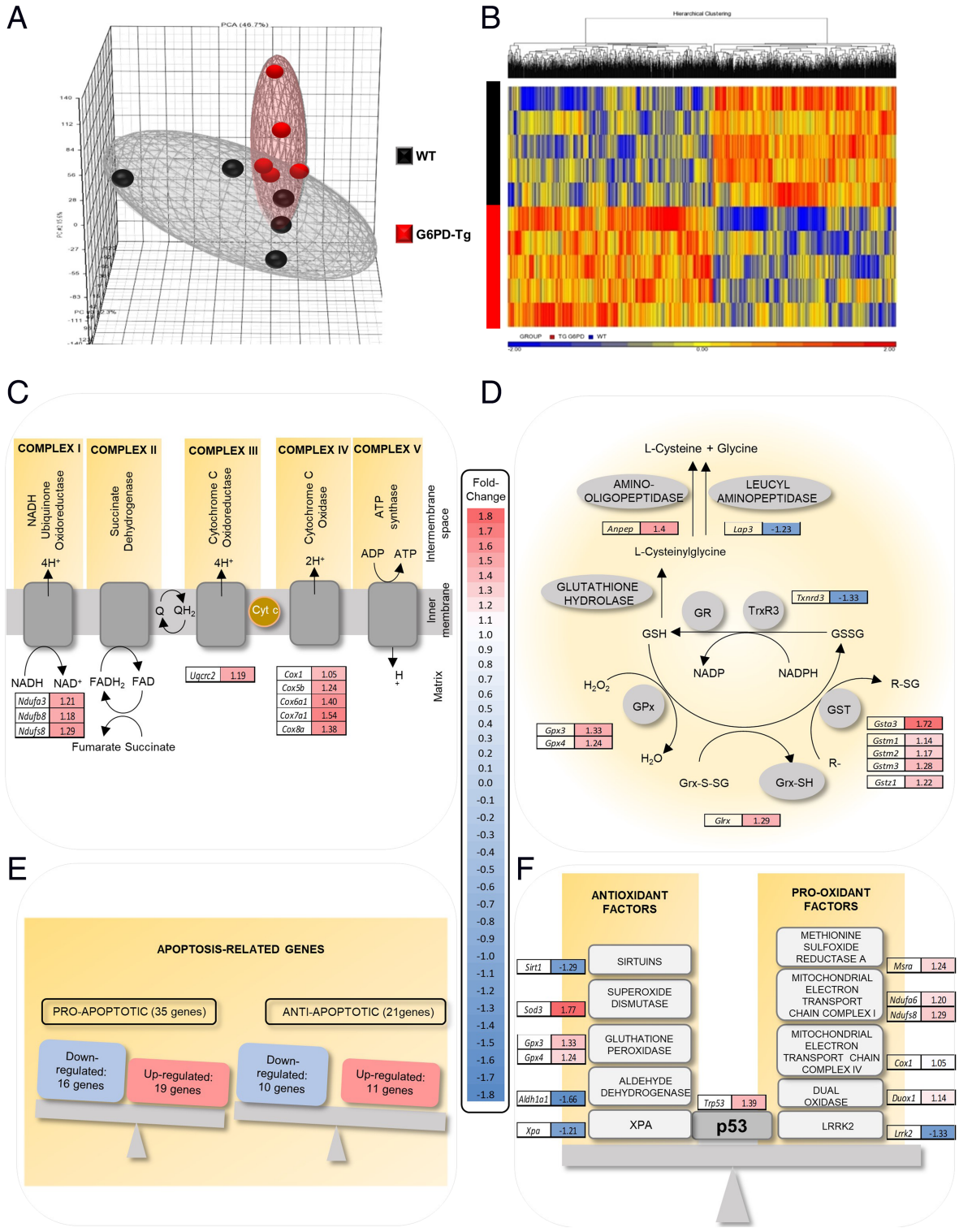

Figure 4 Skeletal muscle transcriptomic analysis in old G6PD-Tg and WT mice. (*A*) Principal component analysis (PCA) showing changes in the transcriptomic profile between 21-month-old G6PD-Tg and WT mice (percentage of variability: 46.7%). (*B*) Unsupervised hierarchical clustering of the 1653 differentially expressed genes in G6PD-Tg and WT samples. (*C*) Genes up-regulated in G6PD-Tg vs. WT from the mitochondrial respiratory chain and oxidative phosphorylation pathway. (*D*) Genes differentially expressed in G6PD-Tg vs. WT from the glutathione metabolism pathway. (*E*) Genes differentially expressed in G6PD-Tg vs. WT from the apoptotic biological process. (*F*) Genes differentially expressed in G6PD-Tg vs. WT from the oxidative stress response biological process. (*C–F*) The fold change is indicated next to the genes' name, and the heatmap for the fold-change values of differently expressed genes is available in the centre of the figure.

Improved reactive oxygen species detoxification in skeletal muscle of G6PD-Tg old mice

Low levels of the reduced (GSH) to oxidized (GSSG) glutathione ratio indicate a lower oxidative stress and improved ROS detoxification.[12] *Figure* 5A shows that the GSH levels were significantly higher (34.5%, $P < 0.01$) whereas those of GSSG (−69%, $P < 0.05$) were significantly lower in the muscles of the G6PD-Tg animals when compared with the WT ones (*Figure* 5B). Consistently, the GSSG/GSH ratio (*Figure* 5C) was significantly lower in the G6PD-Tg group.

We next measured protein carbonylation and two products of lipid peroxidation (MDA and 4-HNE), both markers of ROS-derived damage in 21-month-old WT and G6PD-Tg mice. We did not detect any changes in either MDA levels or protein carbonylation (*Figure* S3), but the levels of 4-HNE were significantly lower (−20.5%, $P < 0.05$) in G6PD-Tg muscles (*Figure* 5D). These results indicate that G6PD overexpression does protect against oxidative stress (glutathione redox ratio) and macromolecular damage through a reduction in the accumulation of oxidized lipids.

Structural and functional impact of glucose 6-P dehydrogenase overexpression in skeletal muscle mitochondria and apoptosis

The impact of G6PD overexpression on mitochondrial morphology and functional adaptations was investigated in skeletal muscle in 21- to 25-month-old WT and 23- to 27-month-old G6PD-Tg animals. We found an increase in the protein levels of cytochrome c oxidase IV (COX IV), one of the nuclear encoded subunits of cytochrome c oxidase (COX IV: 89.7%, $P < 0.05$), in the Tg mice when compared with WT (*Figure* 6A and 6B). This result is consistent with the transcriptomic analysis where we found that five of the nine OXPHOS genes up-regulated in the microarrays in the Tg mice encoded COX subunits (*Table* S2.2). Next, we determined the abundance of mitochondrial OXPHOS complexes in tibialis and gastrocnemius extracts immunoblotted with antibodies specific for protein components of each mitochondrial complex: NADH dehydrogenase (Complex I), succinate dehydrogenase (Complex II), cytochrome b–c1 (Complex III), cytochrome c oxidase (Complex IV), and ATP synthase (Complex

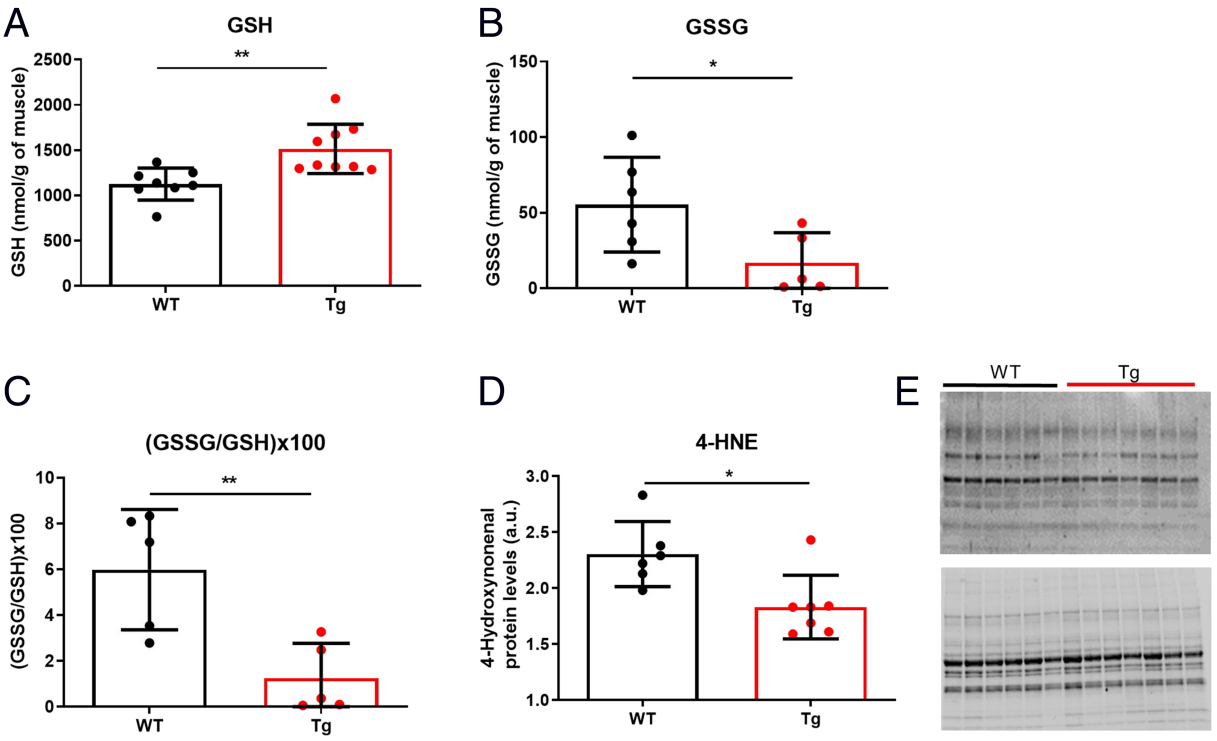

Figure 5 Markers of oxidative stress in muscles of 21-month-old WT and G6PD-Tg mice. (*A*) GSH levels ($n = 8$ WT, $n = 9$ Tg). (*B*) GSSG levels ($n = 6$ WT, $n = 5$ Tg). (*C*) GSSG/GSH×100 ($n = 5$ WT, $n = 5$ Tg). (*D*) Marker of oxidative damage to lipids: 4-HNE levels ($n = 6$ WT, $n = 7$ Tg). (*E*) Membrane representing 4-HNE protein blot (top panel) and its corresponding loading control (bottom panel). Bars represent the mean ± SD. Dots represent individual data. Statistical significance was assessed using the unpaired Student's *t*-test. $^{*}P < 0.05$, $^{**}P < 0.01$.

DOI: 10.1002/jcsm.12792

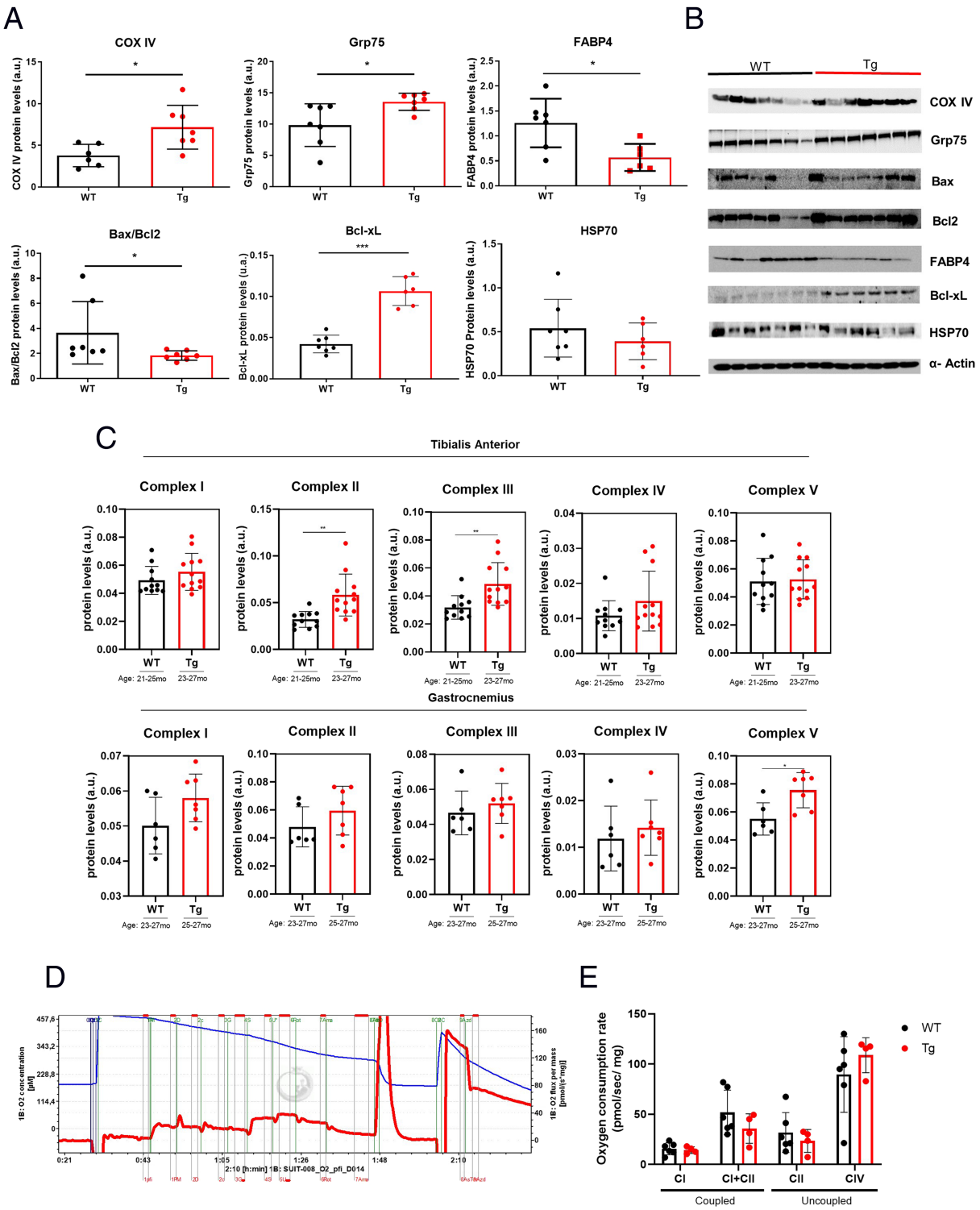

Figure 6 Mitochondrial skeletal muscle parameters in WT and G6PD-Tg animals. (*A*) Protein levels of COX IV (n = 7 WT, n = 7 Tg), Grp75 (n = 7 WT, n = 7 Tg), fatty acid binding protein 4 (FABP4) (n = 6 WT, n = 6 Tg), Bax/Bcl2 (n = 7 WT, n = 7 Tg), Bcl-xL (n = 7 WT, n = 6 Tg), and HSP70 (n = 7 WT, n = 6 Tg) (21-month-old mice). COX IV, Grp75, FABP4, and Bax/Bcl2 were referenced to their stain-free loading control. Bcl-xL and HSP70 were referenced to α-actin. (*B*) Membranes representing COX IV, Grp75, Bax, Bcl2, FABP4, Bcl-xL, HSP70, and α-actin western blots. (*C*) Multi-protein OXPHOS levels determined in tibialis anterior muscle (n = 11 WT, n = 12 Tg) (top panel) and gastrocnemius muscle (n = 6 WT, n = 7 Tg) (bottom panel) (21- to 27-month-old mice). (*D*) Representative image of SUIT 8 Oroboros respiratory experiment. (*E*) Oxygen flow of skeletal muscle bundles (n = 6 WT, n = 4 Tg) (20-month-old mice). Data bars represent the mean ± SD, and dots the individual data. Statistical significance was assessed using the unpaired Student's t-test. $^{*}P < 0.05$, $^{**}P < 0.01$, $^{***}P < 0.001$.

DOI: 10.1002/jcsm.12792

V). G6PD-Tg mice exhibited higher expression of Complex II (81.25%, $P < 0.01$) and Complex III (52.5%, $P < 0.01$) in tibialis and Complex V (37.2%, $P < 0.05$) in gastrocnemius, when compared with the WT (*Figure* 6C). Original gels and stained membranes are shown in *Figure* S4.

Mitochondrial respiration was carried out with permeabilized muscle fibre bundles from soleus muscle in ~20-month-old G6PD-Tg ($n = 4$) and WT mice ($n = 6$) using the Oxygraph-2k. Overexpression of G6PD did not significantly alter the mitochondrial respiration values, although a slightly higher mitochondrial respiration was observed when the Complex IV activity was assayed in the Tg animals when compared with the WT (*Figure* 6D and 6E).

We also determined the protein levels of GRP75 (*Figure* 6A and 6B), a mitochondrial chaperone involved in the refolding of redox-modified proteins.[27] It was significantly increased in the G6PD-Tg compared with WT mice (37.8%, $P < 0.05$). GRP75 is a well-known inhibitor of apoptosis through the modulation of the apoptosis indicator BAX/BCL-2 ratio.[28] The BAX/BCL-2 ratio was also significantly reduced (−25.5%, $P < 0.05$) in the Tg animals (*Figure* 6A and 6B). It was accompanied with an increase in Bcl-xL (20.5%, $P < 0.05$), a member of the Bcl-2 family of proteins that acts as an anti-apoptotic protein. Although we did not find changes in Hsp70 protein levels, a chaperone with anti-apoptotic properties, our results altogether show lower activity of apoptotic processes in mice overexpressing G6PD. These data indicate that G6PD overexpression is associated with an up-regulation of survival/anti-apoptotic factors (*Figure* S2).

To evaluate the accumulation of intramuscular fat, we measured the expression of FABP4,[29] a marker of mature adipocytes, and found significantly lower levels of its expression (−54.7%, $P < 0.05$) in the skeletal muscle of Tg animals when compared with the WT ones (*Figure* 6A and 6B).

Body composition and metabolic measurements in old G6PD-Tg and wild-type mice

Using metabolic cages, we quantified the energy expenditure (EE), the ambulatory activity, and the respiratory exchange ratio (RER) to determine relative use of carbohydrates or lipids for EE in old mice (~20-month-old) (*Figure* 7A, 7C, and 7E).[30] G6PD-Tg animals exhibited lower RER than their WT counterparts indicating oxidation of lipids (WT: L: 0.89 ± 0.03, D: 0.95 ± 0.02; G6PD-Tg: L: 0.77 ± 0.03, D: 0.82 ± 0.02)[31] (*Figure* 7B, *right panel*). The EE-area under the curve (EE-AUC) was also significantly diminished in the Tg mice vs. the WT ones (*Figure* 7D, *right panel*). Moreover, old G6PD-Tg mice exhibited a clear increase in locomotor activity, which, comparatively, was absent in the WT animals (*Figure* 7F, *right panel*).

Using DXA, we did not find changes in body composition (fat, lean, and bone data) (*Figure* S5) or in blood biochemical and haematological parameters that could explain the reported differences as a function of the genotype (*Table* S1).

However, when we assessed the cross-sectional area of muscle fibres from very old mice (34-month-old) (*Figure* 7G and 7H), we found that G6PD-Tg mice had a larger muscle fibre size compared with the WT (1005.5 vs. 901.5 μm^2, respectively, $P < 0.05$). Moreover, we weighted different muscles longitudinally in 6-, 11-, and 23-month-old Tg and WT mice (*Figure* S5b). We found that the percentage of muscle weight lost in gastrocnemius muscle, in 6 vs. 23 months old, was significantly lower in G6PD-Tg when compared with WT mice ($P < 0.004$) (*Figure* 7I).

Exercise training as a physiological intervention to increase glucose 6-P dehydrogenase activity

Exercise training is a cost-effective, clinically proven intervention that can delay and even prevent frailty.[32] We found a significant increase in the mRNA levels of G6PD (127.6%, $P < 0.01$) in C57BL/6J young mice after a short period (5 days) of eccentric exercise training (*Figure* 8A). This was accompanied with a robust increase in the activity of G6PD in skeletal muscle (rest: 0.46 ± 0.16 nmol/min × mg of protein vs. 5 days trained: 1.41 ± 0.78 nmol/min × mg of protein) (*Figure* 8B). Very interestingly, the improvements in the G6PD activity achieved with the exercise training were very similar to that obtained in the mouse harbouring a copy of the complete human G6PD gene (G6PD-Tg: 0.99 ± 0.50 nmol/min × mg of protein, WT: 0.41 ± 0.12 nmol/min × mg of protein; $P < 0.01$) (*Figure* 8C).

Discussion

Delaying the onset of frailty by the overexpression of glucose 6-P dehydrogenase

Frailty has such a relevance in both clinical medicine that finding interventions to delay it is of utmost importance. Several models have been proposed to accelerate the onset of frailty.[8,33] However, to our knowledge, a defined molecular model to delay frailty and promote vigorousness has not yet been proposed. Improvements in 'neuromuscular healthspan' have been reported with resveratrol,[34] caloric restriction,[35] rapamycin,[36] or exercise.[16] Moreover, the HSP70 overexpressing mice[14] and the GHR-KO mice[15] have shown to delay primary sarcopenia or even senescence, but frailty has not been assessed in these models.

The early frailty models were based on the idea that promoting inflammation by knocking-out anti-inflammatory cytokines [such as interleukin (IL)-10] could accelerate the

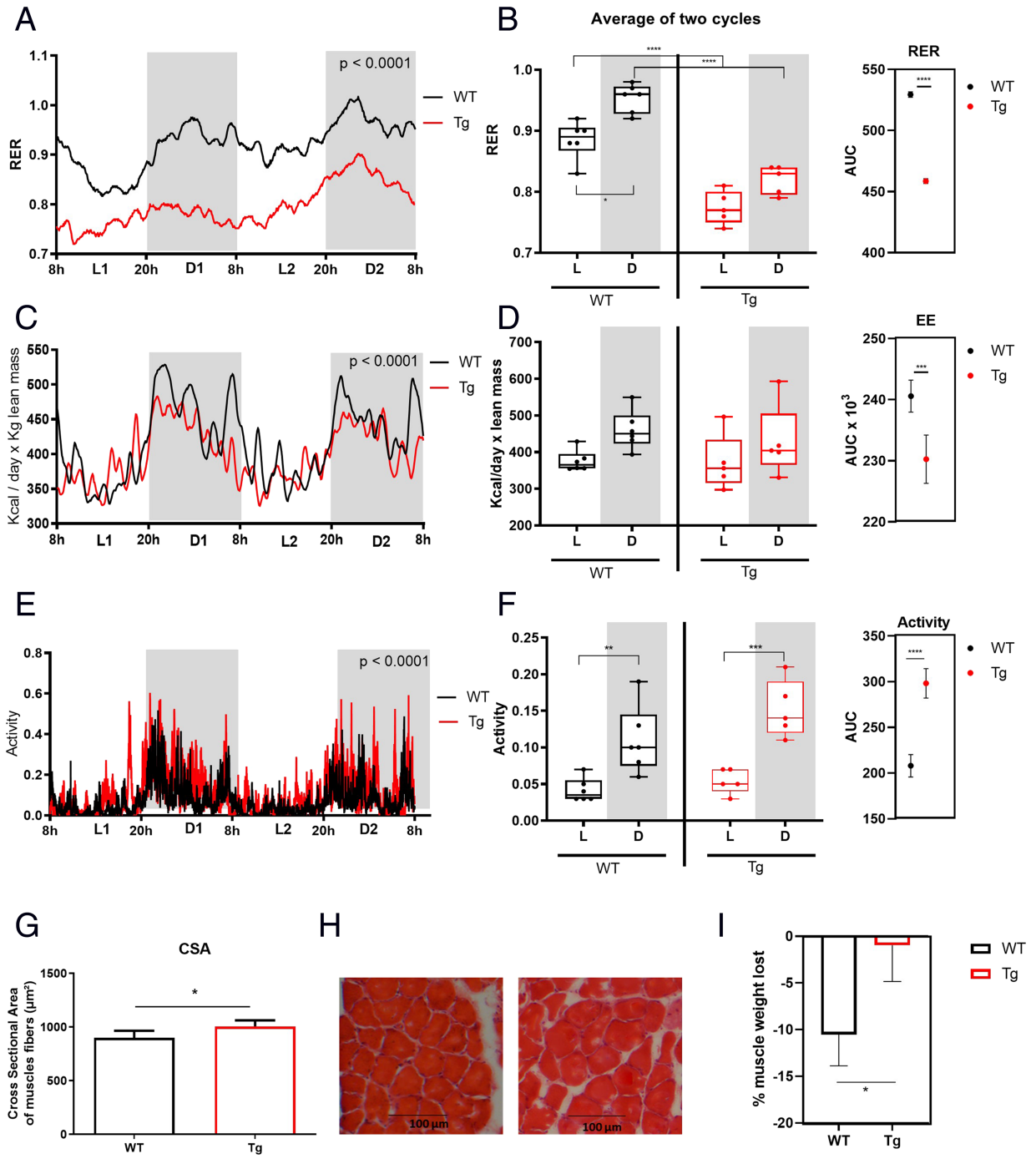

Figure 7 Impact of G6PD overexpression on whole-body skeletal muscle physiology and *in vivo* metabolism in old mice. (*A*) Respiratory exchange ratio over 48 h (RER) (n = 6 WT, n = 5 Tg). (*B*) *(left)* RER average data from the two light (L1 + L2) and dark (D1 + D2) cycles (n = 6 WT, n = 5 Tg). *(right)* Area under the RER curve. (*C*) Energy expenditure (EE) over 48 h (n = 6 WT, n = 5 Tg). (*D*) *(left)* EE average data from the two light (L1 + L2) and dark (D1 + D2) cycles (n = 6 WT, n = 5 Tg). *(right)* Area under the EE curve. (*E*) Voluntary ambulatory activity over 48 h section (n = 6 WT, n = 5 Tg). (*F*) *(left)* Voluntary ambulatory activity average data from the two light (L1 + L2) and dark (D1 + D2) cycles (n = 6 WT, n = 5 Tg). *(right)* Area under the voluntary ambulatory activity curve. (*G*) Cross-sectional area measurement of muscles fibres (μm^2) of very old mice, that is, 34 months of age (n = 8 WT, n = 7 Tg). Data bars represent the mean ± SD. (*H*) Representative images of haematoxylin–eosin colouration used to quantify cross-sectional area. (*I*) Percentage of gastrocnemius muscle weight lost from 6- to 23-month-old G6PD-Tg and WT mice. The effect size has been determined using the *F*-test. $^{**}P < 0.01$. Average data from the two dark and light cycles are represented as box plots with individual values. Mean ± SD area curves are given. Statistical significance was assessed using the unpaired Student's *t*-test, except from panels (*B*), (*D*), and (*F*) *(left)* where statistical significance was assessed using the two-way ANOVA test and panel (*I*) where the effect size has been determined using the *F*-test. $^{*}P < 0.05$, $^{**}P < 0.01$, $^{***}P < 0.001$, $^{****}P < 0.0001$.

DOI: 10.1002/jcsm.12792

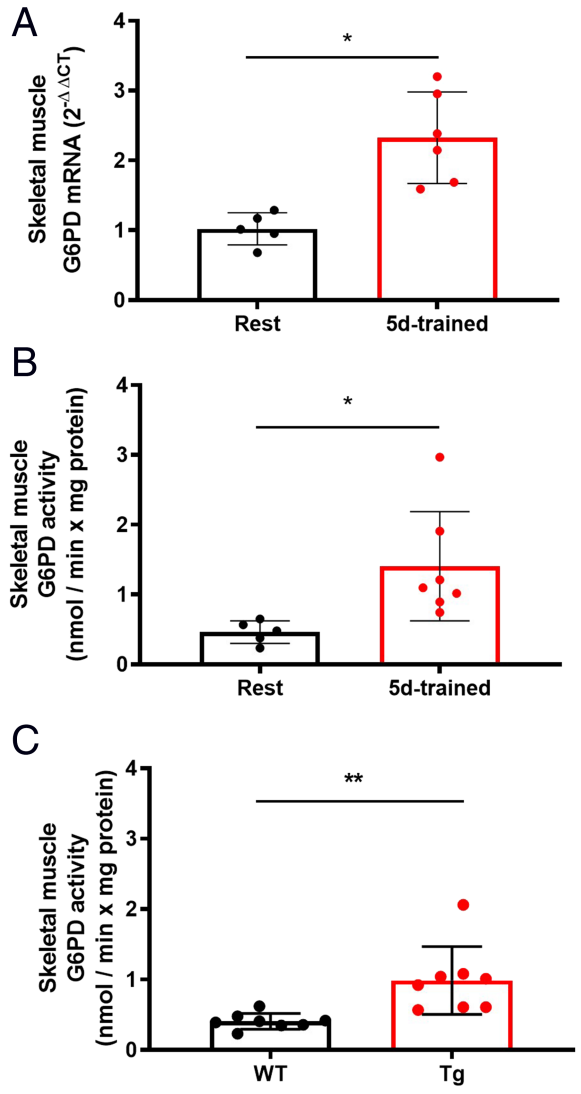

Figure 8 Physical exercise increases G6PD activity and expression. (*A*) G6PD mRNA expression in skeletal muscle from 5 days trained (n = 5) and rest (n = 7) 5-month-old mice. (*B*) G6PD enzymatic activity in skeletal muscle from 5 days trained (n = 5) and rest (n = 7) 5-month-old mice. (*C*) G6PD enzymatic activity in skeletal muscle of WT (n = 8) and Tg (n = 8) 21-month-old mice. Mean ± SD are represented. Dots represent individual data. Statistical significance was assessed using the unpaired Student's t-test. *$P < 0.05$, **$P < 0.01$.

onset of frailty.[8] However, as stated earlier, not one single molecular model has shown to delay the onset of frailty.

Glucose 6-P dehydrogenase is tightly regulated, but we have shown here that it can be modulated by a physiological intervention such as exercise training. We report that only 5 days of eccentric exercise training induces a robust increase in both the mRNA levels and the G6PD activity in skeletal muscle in mice. These increments are similar to those obtained in the G6PD-Tg mice[12] that display a ubiquitous two-fold to four-fold overexpression of G6PD mRNA and also show an equivalent increase in G6PD activity. The exercise-induced increase in the endogenous antioxidant protection may generate a cellular hyper-defensive state being one of the molecular bases of the reported beneficial effects of exercise in the prevention of frailty.[32]

Glucose 6-P dehydrogenase can also be modulated by nutritional and pharmacological interventions.[18–20] Although no medications are available to treat G6PD deficiency, recently, it has been identified a small molecule, AG1, that increases the activity of several common G6PD mutants by improving the binding of $NADP^+$ and/or G6P to the enzyme.[19] AG1 reduces oxidative stress in cells and zebrafish and also decreases diamide-induced oxidative stress in human erythrocytes.[19] AG1 corrects G6PD deficiency but also seems to be suitable to treat subjects with WT G6PD at risk of oxidative stress-related diseases.

Glucose 6-P dehydrogenase-dependent promotion of robustness does not involve improvement in muscle regeneration

We studied the skeletal muscle stem cells regenerative capacity as a possible mechanism that could underlie the observed delay in frailty in the G6PD-Tg mice. Satellite cell regenerative functions decline with aging due to an entry in a senescence state leading to frailty/sarcopenia.[26] G6PD production of NADPH is critical for redox control and cell growth.[25] However, we did not find differences in the regenerative functions of satellite cells from G6PD-Tg and WT animals after muscle injury in any of the ages studied.

Satellite cell-mediated myonuclear accretion has a major role in maturational skeletal muscle growth[37] and during injury-induced skeletal muscle regeneration.[26] However, their contribution to the homeostasis of adult fibres has been an object of debate, and its role in the regulation of muscle mass has been questioned by several experimental evidences.[37] In fact, short-term deletion of satellite cells in adult mice does not result in muscle fibre atrophy, and sarcopenia is generally not exacerbated, reinforcing the notion that satellite cells serve primarily muscle regenerative functions.[38,39] Consistent with this, our results minimize the contribution of muscle satellite cells regenerative potential to the delayed onset of frailty in the G6PD-Tg mice.

In old G6PD-Tg mice, age-associated metabolic changes are prevented

Based on our transcriptomic analysis, we explored several possible mechanisms that could underlie the protective effect of G6PD in terms of frailty. We found a significant decrease in the BAX/BCL-2 ratio and an increase in Bcl-xL in the skeletal muscle of the G6PD-Tg mice, indicating lower activity of apoptotic processes in the animals overexpressing the

antioxidant enzyme. Several signalling pathways of skeletal muscle apoptosis are currently under intense investigation, with a particular focus on the role played by mitochondria. During aging, there is an impairment in cellular mitochondrial function that contributes to muscle atrophy and the decline in muscle performance observed in frail old individuals.[40] This functional decline is associated with substantial reduction in respiratory capacity, ATP production, as well as increased apoptosis.[41] Pathways enriched in genes involved in mitochondrial respiratory chain and mitochondrial genome maintenance are among the most down-regulated ones during aging.[41] In our study, from the nine OXPHOS genes found up-regulated in the microarrays of the G6PD-Tg mice, five of them encoded COX subunits. This result correlates with the higher GRP75 and COX IV levels found in the 21-month-old Tg animals. Poor physical performance in the elderly is associated with a greater decline in mitochondrial respiration as well as COX muscle activity.[42] On the contrary, overexpression of G6PD is associated with a significant increase in the protein levels of COX IV and an improvement in functional parameters in old animals. Consistent with these results, G6PD-Tg mice also exhibited higher expression of Complexes II, III, and V in skeletal muscle, when compared with the WT. Fatty acid oxidation generates $FADH_2$, which is a substrate of Complex II. The up-regulation of Complex II in the Tg animals matches with the indirect calorimetry results. The lower RER-AUC data reveal that old G6PD-Tg animals utilize more lipids than carbohydrates as substrates. Individuals, both humans and rodents, with sedentary lifestyles normally have higher RER values and lower fat oxidation.[30] On the contrary, physically active individuals tend to show lower RER values than untrained ones.[30] Previous studies have shown that old C57BL/6J mice have higher RER levels when compared with young ones, indicating a preference towards carbohydrate utilization. We have also found that the Tg animals show a reciprocal pattern of a lower EE and higher ambulatory activity, indicative of major energetic advantage from an underlying remodelling of gene expression and metabolism in contracting skeletal muscle.

Dysfunctional mitochondria are characterized by an excessive production of ROS, which oxidize and damage macromolecules.[43] We reasoned that the mechanism by which the overexpression of G6PD delays frailty consisted in the alleviation of the load of oxidative damage associated with aging. Indeed, we observed that age-dependent accumulation of oxidized lipids in the skeletal muscle was diminished in the G6PD-Tg mice. This was accompanied with a decrease in the intramuscular adipose tissue levels or fatty acid infiltrations (FABP4) in the Tg animals.[29,44] Our hypothesis was further supported by the observation that the levels of GSH were increased in the transgenic animals while those of the GSSG were significantly decreased in skeletal muscle. Together, these findings reinforce the notion that G6PD delays the onset of frailty by protecting against muscle damage, especially oxidative damage, and not by decreasing muscle regeneration.

We previously showed that oxidative stress is associated with frailty and not with aging itself.[5,45] Support for the idea of the 'free radical theory of frailty' came from a study showing that mice with a deletion of the antioxidant enzyme superoxide dismutase presented signs of muscle weakness, atrophy, and sarcopenia.[7] However, the contrary proposal, that is, that animals protected against oxidative stress could show delayed onset of frailty and increase robustness, had not been tested.

The G6PD-Tg mouse that we describe here is the first defined molecular model to show protection against frailty and promotion of robustness. Our experiments, together with those reported in our previous study,[5] provide support to the idea that damage associated with ROS is involved in the onset of frailty.[2]

Clinical implications

Glucose 6-P dehydrogenase activation increases pentose availability and antioxidant capacity, the former being important in DNA and RNA synthesis and the latter due to the formation of NADPH. This enzyme has several clinical implications. G6PD deficiency is the most common enzyme deficiency in humans.[13] It affects over 400 million people in the world especially in those areas were malaria is common.[13]

In addition to the role of G6PD in preventing haemolysis, the antioxidant properties of this enzyme may relate to development of a variety of other age-associated pathologies, including kidney injury, heart failure, diabetes, and cataracts,[19] suggesting that G6PD deficiency can be an underestimated risk factor for multiple human pathologies and even frailty.

Based on our findings, whether people affected by partial deficiencies of G6PD may be more prone to frailty should be explored in future studies. In view of our results, the activation of the G6PD activity by nutritional,[18] pharmacological,[19] and physiological interventions such as exercise may have translational potential in geriatrics and in gerontological research.

Limitations of the study

The fact that we could not perform all the frailty measurements in every mouse of the Tg and WT cohorts is a limitation of our study especially because it made impossible for us to establish an individual score of frailty. Our model does not allow us to identify pre-frail mice. It only provides us a binary information because we have to identify normal values for each set of mice. The identification of standard physical parameters for each strain of mice would be highly desirable but indeed a daunting task because of the large number of animals required.

Acknowledgements

We thank Dr. Jose Manuel Martí (Berkeley Lab) for his assistance with the digital image acquisition and processing work. We thank Marilyn Noyes for reviewing the English aspects of this work.

The authors of this manuscript certify that they comply with the ethical guidelines for authorship and publishing in the *Journal of Cachexia, Sarcopenia and Muscle*.[46]

Funding

This work was supported by Instituto de Salud Carlos III CB16/10/00435 (CIBERFES) (PID2019-110906RB-I00/AEI/10.13039/501100011033) from the Spanish Ministry of Innovation and Science; 109_RESIFIT from Fundación General CSIC; PROMETEO/2019/097 de 'Consellería, de Sanitat de la Generalitat Valenciana' and EU Funded H2020-DIABFRAIL-LATAM (Ref: 825546); European Joint Programming Initiative 'A Healthy Diet for a Healthy Life' (JPI HDHL); and the ERA-NET Cofund ERA-HDHL (GA No. 696295 of the EU Horizon 2020 Research and Innovation Programme). Part of the equipment employed in this work has been funded by Generalitat Valenciana and co-financed with ERDF funds (OP ERDF of Comunitat Valenciana 2014–2020).

Work in the laboratory of P.J.F.-M. was funded by the FBBVA and the Ramón Areces Foundations. Work in the laboratory of P.M.-C. and A.L.S was funded by by MWRF and Fundació La Marató/TV3-80/19-202021 to P.M.C. and Fundació La Marató de TV3 (Project 202033 to A.L.S.), MINECO-Spain (RTI2018-096068), ERC-2016-AdG-741966, LaCaixa-HEALTH-HR17-00040, MDA, UPGRADE-H2020-825825, AFM, and DPP-Spain; María-de-Maeztu-Program for Units of Excellence to UPF (MDM-2014-0370); and Severo-Ochoa-Program for Centers of Excellence to CNIC (SEV-2015-0505). A.S.-P. was supported by a fellowship from the Spanish 'Ministerio de Educación, Cultura y Deporte', award FPU 14/00098.

Online supplementary material

Additional supporting information may be found online in the Supporting Information section at the end of the article.

Figure S1 related to Figure 1. Functional measurements performed to develop the frailty score in WT and G6PD-Tg mice at four different ages: **(a)** *Body weight,* **(b)** *Activity levels using the* tightrope test*,* **(c)** *Grip strength*, **(d)** *Running time,* and **(e)** *Speed in an incremental treadmill test. Bars represent the mean ± SEM. *p < 0.05, **p < 0.01.*

Figure S2 related to Figure 4. Graphical abstract including the apoptosis-related genes both up-regulated and down-regulated in skeletal muscle in our model**.**

Figure S3 related to Figure 5. Muscle MDA levels and uncropped membranes for carbonylated proteins in muscle samples (n = 8 WT, n = 7 Tg).

Figure S4 related to Figure 6. (a) Expression levels of the multi-protein OXPHOS complexes by immunoblotting in G6PD-Tg (23–27-month-old) and WT (21–25-month-old) mice. (b) Stain-free pictures of representative membranes. The molecular mass of protein standards (in kDa) is shown on the left.

Figure S5 related to Figure 7. (a) X-Ray Absorptiometry Measurements in 20-month-old G6PD-Tg and WT mice in vivo. Lean mass, fat mass, fat in tissue, and bone mineral density. (b) Gastrocnemius and soleus muscle weight in 6-month-old, 11-month-old, and 23-month-old G6PD-Tg and WT mice.

Table S1 related to Figure 7. Main blood biochemical and hematological parameters in ~20-month-old G6PD-Tg and WT mice.

Table S2 related to Figure 4.

Table S2.1. Specific metabolic pathways and biological processes in terms of enrichment. *P*-value derived from the 1,653 significant genes using Pathway Studio.

Table S2.2. Complete list of genes involved in the metabolic pathways and biological processes shown in table 1.1. *P*-value and fold-change refer to the comparison between G6PD-Tg vs WT mice.

Data S1. Supporting information.

Conflict of interests

The authors declare no competing financial interests.

References

1. Vina J, Tarazona-Santabalbina FJ, Perez-Ros P, Martinez-Arnau FM, Borras C, Olaso-Gonzalez G, et al. Biology of frailty: modulation of ageing genes and its importance to prevent age-associated loss of function. *Mol Aspects Med* 2016;**50**:88–108.
2. Vina J, Borras C, Gomez-Cabrera MC. A free radical theory of frailty. *Free Radic Biol Med* 2018;**124**:358–363.
3. Fried LP, Tangen CM, Walston J, Newman AB, Hirsch C, Gottdiener J, et al. Frailty in older adults: evidence for a phenotype. *J Gerontol A Biol Sci Med Sci* 2001;**56**: M146–M156.

4. Matheu A, Maraver A, Klatt P, Flores I, Garcia-Cao I, Borras C, et al. Delayed ageing through damage protection by the Arf/p53 pathway. *Nature* 2007;**448**:375–379.
5. Ingles M, Gambini J, Carnicero JA, Garcia-Garcia FJ, Rodriguez-Manas L, Olaso-Gonzalez G, et al. Oxidative stress is related to frailty, not to age or sex, in a geriatric population: lipid and protein oxidation as biomarkers of frailty. *J Am Geriatr Soc* 2014;**62**:1324–1328.
6. Saum KU, Dieffenbach AK, Jansen EH, Schottker B, Holleczek B, Hauer K, et al. Association between oxidative stress and frailty in an elderly German population: results from the ESTHER cohort study. *Gerontology* 2015;**61**:407–415.
7. Deepa SS, Bhaskaran S, Espinoza S, Brooks SV, McArdle A, Jackson MJ, et al. A new mouse model of frailty: the Cu/Zn superoxide dismutase knockout mouse. *Geroscience* 2017;**39**:187–198.
8. Walston J, Fedarko N, Yang H, Leng S, Beamer B, Espinoza S, et al. The physical and biological characterization of a frail mouse model. *J Gerontol A Biol Sci Med Sci* 2008;**63**:391–398.
9. Ghergurovich JM, García-Cañaveras JC, Wang J, Schmidt E, Zhang Z, TeSlaa T, et al. A small molecule G6PD inhibitor reveals immune dependence on pentose phosphate pathway. *Nat Chem Biol* 2020;**16**:731–739.
10. Fernandez-Marcos PJ, Nobrega-Pereira S. NADPH: new oxygen for the ROS theory of aging. *Oncotarget* 2016;**7**:50814–50815.
11. Legan SK, Rebrin I, Mockett RJ, Radyuk SN, Klichko VI, Sohal RS, et al. Overexpression of glucose-6-phosphate dehydrogenase extends the life span of *Drosophila melanogaster*. *J Biol Chem* 2008;**283**:32492–32499.
12. Nóbrega-Pereira S, Fernandez-Marcos PJ, Brioche T, Gomez-Cabrera MC, Salvador-Pascual A, Flores JM, et al. G6PD protects from oxidative damage and improves healthspan in mice. *Nat Commun* 2016;**7**:10894.
13. Cappellini MD, Fiorelli G. Glucose-6-phosphate dehydrogenase deficiency. *Lancet* 2008;**371**:64–74.
14. Broome CS, Kayani AC, Palomero J, Dillmann WH, Mestril R, Jackson MJ, et al. Effect of lifelong overexpression of HSP70 in skeletal muscle on age-related oxidative stress and adaptation after nondamaging contractile activity. *FASEB J* 2006;**20**:1549–1551.
15. Arum O, Rickman DJ, Kopchick JJ, Bartke A. The slow-aging growth hormone receptor/binding protein gene-disrupted (GHR-KO) mouse is protected from aging-resultant neuromusculoskeletal frailty. *Age (Dordr)* 2014;**36**:117–127.
16. Gomez-Cabrera MC, Garcia-Valles R, Rodriguez-Manas L, Garcia-Garcia FJ, Olaso-Gonzalez G, Salvador-Pascual A, et al. A new frailty score for experimental animals based on the clinical phenotype: inactivity as a model of frailty. *J Gerontol A Biol Sci Med Sci* 2017;**72**:885–891.
17. Martinez de Toda I, Garrido A, Vida C, Gomez-Cabrera MC, Vina J, De la Fuente M. Frailty quantified by the "Valencia Score" as a potential predictor of lifespan in mice. *J Gerontol A Biol Sci Med Sci* 2018;**73**:1323–1329.
18. Katare R, Caporali A, Emanueli C, Madeddu P. Benfotiamine improves functional recovery of the infarcted heart via activation of pro-survival G6PD/Akt signaling pathway and modulation of neurohormonal response. *J Mol Cell Cardiol* 2010;**49**:625–638.
19. Hwang S, Mruk K, Rahighi S, Raub AG, Chen CH, Dorn LE, et al. Correcting glucose-6-phosphate dehydrogenase deficiency with a small-molecule activator. *Nat Commun* 2018;**9**:4045.
20. Brioche T, Kireev RA, Cuesta S, Gratas-Delamarche A, Tresguerres JA, Gomez-Cabrera MC, et al. Growth hormone replacement therapy prevents sarcopenia by a dual mechanism: improvement of protein balance and of antioxidant defenses. *J Gerontol A Biol Sci Med Sci* 2014;**69**:1186–1198.
21. Suelves M, Vidal B, Serrano AL, Tjwa M, Roma J, López-Alemany R, et al. uPA deficiency exacerbates muscular dystrophy in MDX mice. *J Cell Biol* 2007;**178**:1039–1051.
22. Giustarini D, Dalle-Donne I, Milzani A, Fanti P, Rossi R. Analysis of GSH and GSSG after derivatization with *N*-ethylmaleimide. *Nat Protoc* 2013;**8**:1660–1669.
23. Ingles M, Serra-Ano P, Gambini J, Abu-Sharif F, Dromant M, Garcia-Valles R, et al. Active paraplegics are protected against exercise-induced oxidative damage through the induction of antioxidant enzymes. *Spinal Cord* 2016;**54**:830–837.
24. Waller HD, Lohr GW, Tabatabai M. Hemolysis and absence of glucose-6-phosphate dehydrogenase in erythrocytes; an enzyme abnormality of erythrocytes. *Klin Wochenschr* 1957;**35**:1022–1027.
25. Wagner KR, Kauffman FC, Max SR. The pentose phosphate pathway in regenerating skeletal muscle. *Biochem J* 1978;**170**:17–22.
26. Sousa-Victor P, Gutarra S, García-Prat L, Rodriguez-Ubreva J, Ortet L, Ruiz-Bonilla V, et al. Geriatric muscle stem cells switch reversible quiescence into senescence. *Nature* 2014;**506**:316–321.
27. Deocaris CC, Kaul SC, Wadhwa R. On the brotherhood of the mitochondrial chaperones mortalin and heat shock protein 60. *Cell Stress Chaperones* 2006;**11**:116–128.
28. Chelh I, Meunier B, Picard B, Reecy MJ, Chevalier C, Hocquette JF, et al. Molecular profiles of Quadriceps muscle in myostatin-null mice reveal PI3K and apoptotic pathways as myostatin targets. *BMC Genomics* 2009;**10**:196.
29. Pagano AF, Brioche T, Arc-Chagnaud C, Demangel R, Chopard A, Py G. Short-term disuse promotes fatty acid infiltration into skeletal muscle. *J Cachexia Sarcopenia Muscle* 2018;**9**:335–347.
30. McMullan RC, Kelly SA, Hua K, Buckley BK, Faber JE, Pardo-Manuel de Villena F, et al. Long-term exercise in mice has sex-dependent benefits on body composition and metabolism during aging. *Physiol Rep* 2016;**4**:e13011.
31. Houtkooper RH, Argmann C, Houten SM, Canto C, Jeninga EH, Andreux PA, et al. The metabolic footprint of aging in mice. *Sci Rep* 2011;**1**:134.
32. Tarazona-Santabalbina FJ, Gomez-Cabrera MC, Perez-Ros P, Martinez-Arnau FM, Cabo H, Tsaparas K, et al. A multicomponent exercise intervention that reverses frailty and improves cognition, emotion, and social networking in the community-dwelling frail elderly: a randomized clinical trial. *J Am Med Dir Assoc* 2016;**17**:426–433.
33. Jurk D, Wilson C, Passos JF, Oakley F, Correia-Melo C, Greaves L, et al. Chronic inflammation induces telomere dysfunction and accelerates ageing in mice. *Nat Commun* 2014;**2**:4172.
34. Kane AE, Hilmer SN, Boyer D, Gavin K, Nines D, Howlett SE, et al. Impact of longevity interventions on a validated mouse clinical frailty index. *J Gerontol A Biol Sci Med Sci* 2016;**71**:333–339.
35. Brandhorst S, Choi IY, Wei M, Cheng CW, Sedrakyan S, Navarrete G, et al. A periodic diet that mimics fasting promotes multi-system regeneration, enhanced cognitive performance, and healthspan. *Cell Metab* 2015;**22**:86–99.
36. Correia-Melo C, Birch J, Fielder E, Rahmatika D, Taylor J, Chapman J, et al. Rapamycin improves healthspan but not inflammaging in $nf\kappa b1^{-/-}$ mice. *Aging Cell* 2018;**18**:e12882.
37. Murach KA, Fry CS, Kirby TJ, Jackson JR, Lee JD, White SH, et al. Starring or supporting role? Satellite cells and skeletal muscle fiber size regulation. *Physiology (Bethesda)* 2018;**33**:26–38.
38. Lepper C, Partridge TA, Fan CM. An absolute requirement for Pax7-positive satellite cells in acute injury-induced skeletal muscle regeneration. *Development* 2011;**138**:3639–3646.
39. Sambasivan R, Yao R, Kissenpfennig A, Van Wittenberghe L, Paldi A, Gayraud-Morel B, et al. Pax7-expressing satellite cells are indispensable for adult skeletal muscle regeneration. *Development* 2011;**138**:3647–3656.
40. Derbre F, Gomez-Cabrera MC, Nascimento AL, Sanchis-Gomar F, Martinez-Bello VE, Tresguerres JA, et al. Age associated low mitochondrial biogenesis may be explained by lack of response of PGC-1α to exercise training. *Age (Dordr)* 2011;**34**:669–679.
41. Gonzalez-Freire M, de Cabo R, Bernier M, Sollott SJ, Fabbri E, Navas P, et al. Reconsidering the role of mitochondria in aging. *J Gerontol A Biol Sci Med Sci* 2015;**70**:1334–1342.
42. Joseph AM, Adhihetty PJ, Buford TW, Wohlgemuth SE, Lees HA, Nguyen LM, et al. The impact of aging on mitochondrial function and biogenesis pathways in skeletal muscle of sedentary high- and low-functioning elderly individuals. *Aging Cell* 2012;**11**:801–809.

43. Viña J, Olaso-Gonzalez G, Arc-Chagnaud C, De la Rosa A, Gomez-Cabrera MC. Modulating oxidant levels to promote healthy aging. *Antioxid Redox Signal* 2020;**33**:570–579.
44. Sathyan S, Ayers E, Gao T, Milman S, Barzilai N, Verghese J. Plasma proteomic profile of frailty. *Aging Cell* 2020;**19**: e13193.
45. Viña J, Borras C, Gomez-Cabrera MC. A free radical theory of frailty. *Free Radic Biol Med* 2018;**124**:358–363.
46. von Haehling S, Morley JE, Coats AJS, Anker SD. Ethical guidelines for publishing in the *Journal of Cachexia, Sarcopenia and Muscle*: update 2019. *J Cachexia Sarcopenia Muscle* 2019;**10**:1143–1145.